



## Effect of using phase change material (PCM) magnesium sulfate ( $MgSO_4$ ) solution as heat storage in solar powered thermoelectric cooler box

D. Priyuko, Rifky\*, A. Saputra, A.I. Fahrezi, M.I. Sobirin

Jurusan Teknik Mesin, Fakultas Teknologi Industri dan Informatika, Universitas Muhammadiyah Prof. DR. HAMKA, Jl. Tanah Merdeka no.6 Rambutan Ciracas Jakarta Timur, DKI Jakarta, Indonesia.

\*E-mail: [rifky@uhamka.ac.id](mailto:rifky@uhamka.ac.id)

### ARTICLE INFO

### ABSTRACT

#### Article History:

Received 31 August 2024

Accepted 24 March 2025

Available online 01 April 2025

#### Keywords:

Photovoltaic

Thermoelectric

PCM

Cooler box



Utilization of new, renewable energy sources is very important for society as a way to switch from fossil fuels. Solar energy is a type of renewable energy that is very promising for various applications. Traditional cooling systems contribute to the depletion of the ozone layer, requiring alternatives such as using thermoelectric solar energy (TEC) for cooling. In addition, PCM used, such as 25%, 30%, and 35%  $MgSO_4$  solutions, can absorb latent heat during the cooling process, thereby increasing efficiency. This research aims to increase coefficient of performance (CoP) of cooling boxes by integrating solar energy and PCM. Data collection was carried out from 09.30 to 14.40, by measuring light intensity, voltage and current, solar panel temperature, environmental temperature, cooler box wall temperature and TEC temperature. Over three days of data collection, this study determined the minimum temperature and CoP for the cooler. The findings show that the minimum temperature in the cooler without PCM is 16.8°C. Coolers with PCM  $MgSO_4$ , 25%, 30%, and 35% the minimum temperatures are 16.7°C, 12.7°C, and 14.7°C. Regarding the average COP, the cooling box without PCM reached 0.0345, while the box with 25%, 30%, and 35% PCM  $MgSO_4$  had a CoP of 0.0354, 0.0469, and 0.0402, respectively. The study concluded that 30%  $MgSO_4$  PCM solution is most suitable for use as PCM, because it affects the minimum temperature and COP of the cooling system. This effectiveness is due to the concentration of  $MgSO_4$  lowering the freezing point of the solution, thereby increasing the cooling performance.

## 1. INTRODUCTION

The use of new renewable energy can be a concern among Indonesian people to slowly reduce the use of fossil energy, which is also to protect this earth. In its application, solar energy has the potential to meet adequate energy needs. Durganjali et al. (2020). Solar energy is an energy that is clean and environmentally friendly in its use. Solar energy transferred to the Indonesian earth will always exist throughout the year, it is estimated that the ability of sunlight in the country of Indonesia is  $0.9 \times 10^8$  kJ / year. Silaban et al. (2013). However, the utilization of solar energy requires media to be able to convert and store solar energy, which will produce output in the form of electrical energy.

Electrical energy can be generated from the direct conversion of solar light energy in photovoltaic (PV) systems, which often receive attention from researchers because PV systems are free of carbon emissions, environmentally friendly and easily available due to their abundant sources. Durganjali et al. (2020).

Solar panels consist of multiple solar cells arranged to achieve the expected output power and performance. When grouped together, the solar cells' capability is that sunlight can be converted into direct electric current (Harahap, 2020). The voltage and current produced by solar cells are affected by two physical variables, sunlight intensity and ambient temperature. Suryana et al. (2016). The efficiency of a solar panel depends on three factors: the level of solar radiation flux, the quality of the semiconductors used, and the operating temperature of the solar panel. Biwole et al. (2011). The way a PV system or solar cell works is by utilizing sunlight as particles, which are called photons. Salsa Hayani et al. (2021). In utilizing solar modules more widely, they can be used to supply electricity to thermoelectrics. Fikry et al. (2024).

Thermoelectric module is a module that can convert electrical energy and convert it into cold or hot temperatures made of semiconductor materials. Puspita et al. (2017). The thermoelectric module refers to the Peltier effect principle where heat exchange occurs at the junction of two dissimilar metals when an electric current flows which functions as a heat pump that conducts heat from the cold side to the hot side. Sharpe et al. (2020).

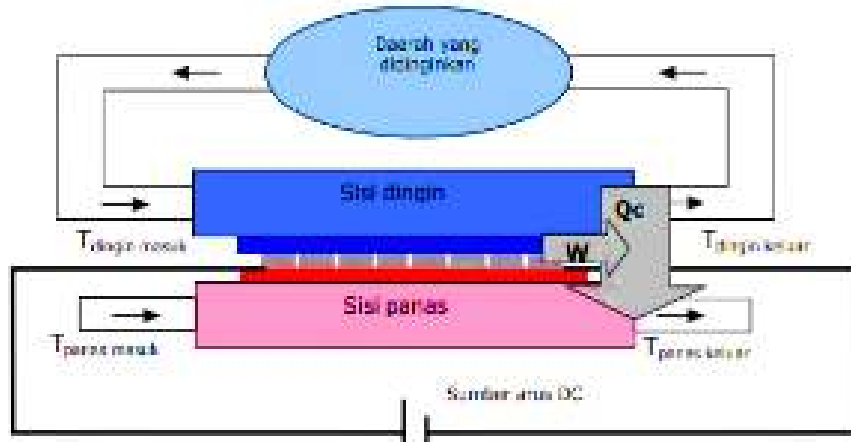


Figure 1. Schematic of how thermoelectric works

The thermoelectric effect, which is the basis for energy conversion, can be effectively illustrated by referring to a schematic thermocouple. In the operational diagram of a thermoelectric air conditioner, the cooling process occurs when the air inside the cooled area passes through the cold side of the circulating heatsink inside. Meanwhile, heat from the hot side is released as air flows across the hot side of the heatsink. Akbar et al. (2021). In addition, a phase change material (PCM) is also used in the cooler box.

PCM is a 'latent' heat storage material that uses chemical bonds to store and release heat. Tyagi et al. (2007). PCM is used as a replacement for main memory which has sufficient endurance. Ferreira et al. (2010). Another advantage of the PCM is that in performing a phase change the temperature is almost always constant. Pomianowski et al. (2013). The PCM is made from magnesium sulfate (MgSO<sub>4</sub>), a salt hydrate that has a high latent heat and conventional melting temperature to absorb latent heat during the cooling process to make it more efficient. Khandagre et al. (2021).

There has been a lot of research on thermoelectrics including those used for cooling systems in car cabins, medical cooler boxes. Other research has been on different heat storage materials as phase change materials but those using phase change materials in refrigeration such as magnesium sulfate have not been much or very little research available. Rifky et al. (2020), Salsabila et al. (2021), Vasanthkumar et al. (2014). Therefore, this research tries to optimize the cooling box by adding PCM made from MgSO<sub>4</sub> in it, which aims to get the effect

of adding PCM made from  $MgSO_4$  on the minimum temperature achievement of the cooling box and the cooling system performance coefficient.

## 2. RESEARCH METHODS

This study used a box-shaped container with Styrofoam material measuring 30 cm x 21 cm x 25 cm, using 50 Wp Polycrystalline solar modules, eight TEC 1-12706 modules assembled in series, mounted on the inner and outer heatsinks with the help of four fans in each box as a heat dissipator. The study was conducted experimentally to determine the lowest temperature of the four cooling boxes achieved by varying the cooling box without PCM and the cooling box using 25%  $MgSO_4$  PCM, 30%  $MgSO_4$  PCM, and 35%  $MgSO_4$  PCM. The cooling box construction design can be seen in Figure 2 below.



Figure 2. (a) Cooling box without PCM (b) Cooling box using PCM

The cooling system also uses PCM which is placed on the inside of the cooling box. Here is a picture of the  $MgSO_4$  PCM that has been placed in an ice pack with a capacity of 500 ml.



Figure3. PCM  $MgSO_4$  with  $MgSO_4$  25%,  $MgSO_4$  30%,  $MgSO_4$  35% composition

The picture above shows each PCM of different  $MgSO_4$  solutions, namely in PCM  $MgSO_4$  25% consists of a composition of 125 grams of  $MgSO_4$  and 375 grams of  $H_2O$ , PCM  $MgSO_4$  30% consists of a composition of 150 grams of  $MgSO_4$  and 350 grams of  $H_2O$ , and PCM  $MgSO_4$  35% consists of a composition of 175 grams of  $MgSO_4$  and 325 grams of  $H_2O$ . Meanwhile, the dimensions of the wall area on the outside and inside walls that have been installed heatsinks on the right and left sides with an area of  $0.004 \text{ m}^2$ , while the other side of the wall as is. The design of the thermoelectric module circuit can be seen in Figure 4 below.

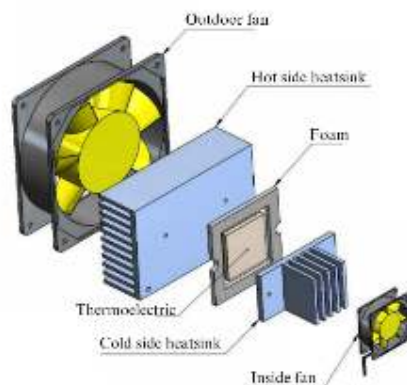


Figure4. Thermoelectric module circuit

The thermoelectric module circuit located between the heatsink aims to distribute the temperature on the hot side and cold side thermoelectrics. While the fan helps to release heat and accelerate the cooling process of the thermoelectric. The coating material consisting of aluminum foil and styrofoam is shown in the figure.

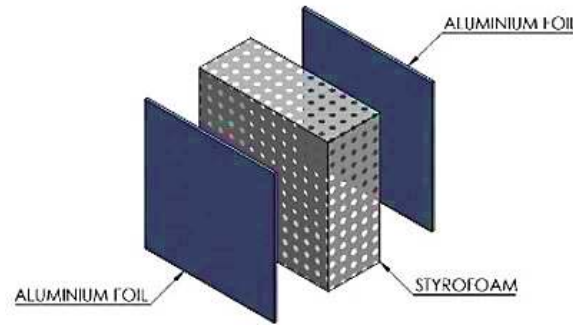


Figure5. Cooling box lining material

Meanwhile, on the cooler box there is a wall symbol as shown below.

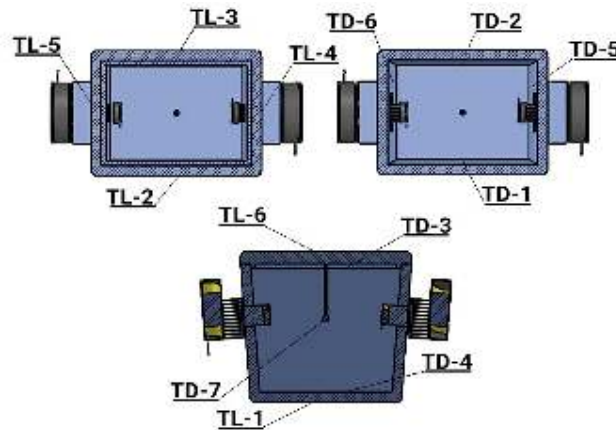


Figure 6. Location of temperature measurement on the cooler box

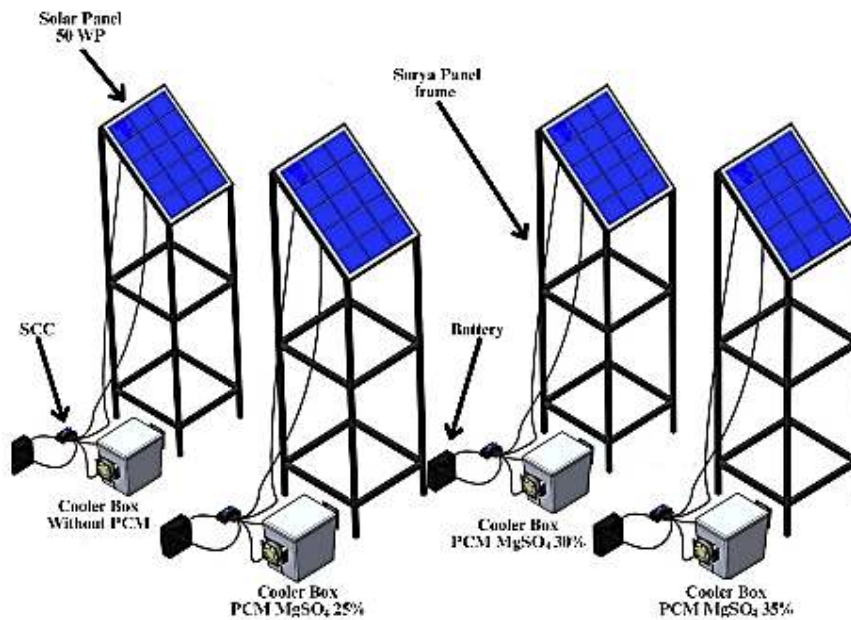


Figure7. Cooling system circuit design

Figure 6 shows the location of the temperature in the cooler box which consists of the temperature of the inner wall of the cooler box and the temperature of the outer wall of the cooler box. At the inner temperature,

namely: TD-1 = temperature in front, TD-2 = temperature in the back, TD-3 = temperature in the top, TD-4 = temperature in the bottom, TD-5 = temperature in the right, TD-6 = temperature in the left, and TD-7 = temperature in the middle room. While at the outside temperature of the cooler box, namely: TL-1 = bottom outside temperature, TL-2 = front outside temperature, TL-3 = rear outside temperature, TL-4 = right outside temperature, TL-5 = left outside temperature, and TL-6 = top outside wall temperature. The tools used in this study can be seen in the series of images, figure 7.

In figure 7, the solar module is connected to a watt meter to determine the electrical power provided and then proceed to the SCC. SCC is used to regulate the current to the load and regulate battery charging. After that, the current regulated by the SCC is given to the TEC load through the watt meter. The method of data collection carried out in this study is by taking measurements.

The efficiency of solar cells is influenced by the material properties of the cells and external factors such as ambient temperature, light intensity, and the range of light entering the solar panel. This research focuses on measuring and calculating the input of electrical power from the intensity of sunlight using the following equation. Rifky et al. (2020):

$$P_m = I_r A \quad (1)$$

The heat transfer rate that occurs in the thermoelectric cooler box is conduction and convection heat transfer. Heat transfer transfers energy to a solid material or fluid that is not moving due to a temperature difference. Rifky et al.(2020), Maulani et al.(2023). Convection transfer is a method of transferring energy originating from a surface whose temperature is higher than its environment. It involves the transportation of energy along a temperature gradient due to the movement of most particles in the flowing substance. Akbar et al. (2023).

In convection heat transfer, there are four numbers that have no units, namely Prandtl number (Pr), Nusselt number (Nu), Grashof number (Gr), and Rayleigh number (Ra). The Nusselt number can be seen in the following equation. Rifky et al.(2020).

$$Nu_x = \frac{hx}{k} \quad (2)$$

Calculation of free convection on each cooling box wall is used to find the heat load transmission between the inner wall and the outside environment. The equation can be seen as follows. Rifky et al. (2020).

$$Gr_x = \frac{g \cdot \beta \cdot (T_w - T_\infty) \cdot x^3}{\nu^2} \quad (3)$$

$$T_f = \frac{(T_w - T_\infty)}{2} \quad (4)$$

$$Ra = Gr \cdot Pr \quad (5)$$

Meanwhile, free convection on a vertical plate is determined by the following two equations. Rifky et al. (2020).

$$\overline{Nu} = 0,68 + \frac{0,670 Ra^{1/4}}{\left[1 + \left(\frac{0,492}{Pr}\right)^{9/16}\right]^{8/27}} \text{ untuk } Ra_L < 10^9 \quad (6)$$

$$\overline{Nu}^{1/2} = 0,825 + \frac{0,387 Ra^{1/6}}{\left[1 + \left(\frac{0,492}{Pr}\right)^{9/16}\right]^{8/27}} \text{ untuk } 10^{-1} < Ra_L < 10^{12} \quad (7)$$

Furthermore, when you want to know forced convection, calculate the Reynolds number (Re) to determine whether the water is laminar or turbulent. The Re equation can be seen as follows. Cengel et al. (2015).

$$Re = \frac{\text{Inertia Forces}}{\text{Viscous}} = \frac{\rho \cdot V \cdot L_c \cdot V \cdot L_c}{\mu \cdot \nu} \quad (8)$$

In forced convection, the Nusselt number (Nu) also applies to measure the effectiveness of heat transfer which is also seen based on laminar or turbulent flow conditions. The equation is as follows. Cengel et al.(2015).

Laminar

$$Nu \frac{hL}{k} = 0,664 \cdot Re^{0,5} \cdot Pr^{\frac{1}{3}} \rightarrow Re < 5 \times 10^5, Pr > 0,6 \quad (9)$$

Turbulent

$$Nu \frac{hL}{k} = 0,037 \cdot Re^{0,8} \cdot Pr^{\frac{1}{3}} \rightarrow 5 \times 10^5, \leq Re \leq 10^7, 0,6 \leq Pr \leq 60 \quad (10)$$

The lost heat load ( $q_2$ ) is the load that comes from outside the cooler box, where the wall in the cooler box has a cooling load value. Setiawan et al(2019).The lost heat load can be seen in the following equation.

$$q_1 = \frac{T \cdot l - T \cdot rp}{\left(\frac{\Delta x_1}{k_{1.A_1}}\right) + \left(\frac{\Delta x_2}{k_{2.A_2}}\right) + \left(\frac{\Delta x_3}{k_{3.A_3}}\right)} \quad (11)$$

Transmission heat load ( $q_2$ ) is the event of heat loss due to the temperature difference on both sides of the element, and can be calculated using the following equation. Susilo et al.(2020).

$$q_2 = U \cdot A \cdot \Delta T \quad (12)$$

Where  $U$  is the total heat transfer coefficient of the convection process coefficient (W/m<sup>2</sup>. K),  $A$  is the surface area (m<sup>2</sup>), and  $\Delta T$  indicates the temperature difference.

Furthermore, when you want to know the value of the heat transfer coefficient, it can be seen in the following equation. Setiawan et al.(2019).

$$U = \frac{1}{\left[\frac{1}{h_{in}} + \frac{\Delta x_{AL}}{k_{AL}} + \frac{\Delta x_{Sty}}{k_{Sty}} + \frac{\Delta x_{AL}}{k_{AL}} + \frac{1}{h_{out}}\right]} \quad (13)$$

The total heat load of the cooler ( $q_c$ ) is obtained from the summation of the heat loss and heat transmission load found in the following equation.

$$q_c = q_1 + q_2 \quad (14)$$

The coefficient of performance (CoP) is the value of the thermoelectric cooling system. CoP is calculated with the following equation.Rifky et al.(2020).

$$CoP = \frac{q_c}{p_{in}} \quad (15)$$

### 3. RESULTS AND DISCUSSION

Test data and calculations carried out with four variations, namely the cooler box without PCM, 25% PCM MgSO<sub>4</sub> cooler box, 30% PCM MgSO<sub>4</sub> cooler box, 35% PCM MgSO<sub>4</sub> cooler box, obtained the minimum temperature measurement results of the cooler box obtained from the average temperature of each cooler box. The following is the minimum temperature of the cooler box shown in the table below.

Table 1. Temperature of the cooler box for three days

No.	Posision	Minimum temperature of the cooler box chamber(°C)			
		Without PCM	MgSO <sub>4</sub> 25%	MgSO <sub>4</sub> 30%	MgSO <sub>4</sub> 35%
1	TD-1	17.9	18.1	17.2	15.7
2	TD-2	17.5	17.7	15.8	15.8
3	TD-3	18.2	17.7	16.9	15.6
4	TD-4	17.7	19.5	18.7	17.3
5	TD-5	18.3	17.2	16.6	15.3
6	TD-6	17.8	18.3	16.7	15.6
7	TD-7	16.8	16.7	12.7	14.7
Minimum		16.8	16.7	12.7	14.7

Maximum	18.3	19.5	18.7	17.3
---------	------	------	------	------

Table 1 shows the results of temperature measurements on the inside of the cooler box for three days. The minimum temperature obtained in the cooler box room for three days was 12.7°C, which occurred in the cooler box using PCM MgSO<sub>4</sub> 30% at TD-7, while the maximum temperature obtained on the second day was in the cooler box using PCM MgSO<sub>4</sub> 25% at 19.5°C which occurred at TD-4.

To facilitate analysis, the data is presented in graphical form. This graph illustrates the minimum temperature distribution on each wall of the box which can be seen in the figure below.

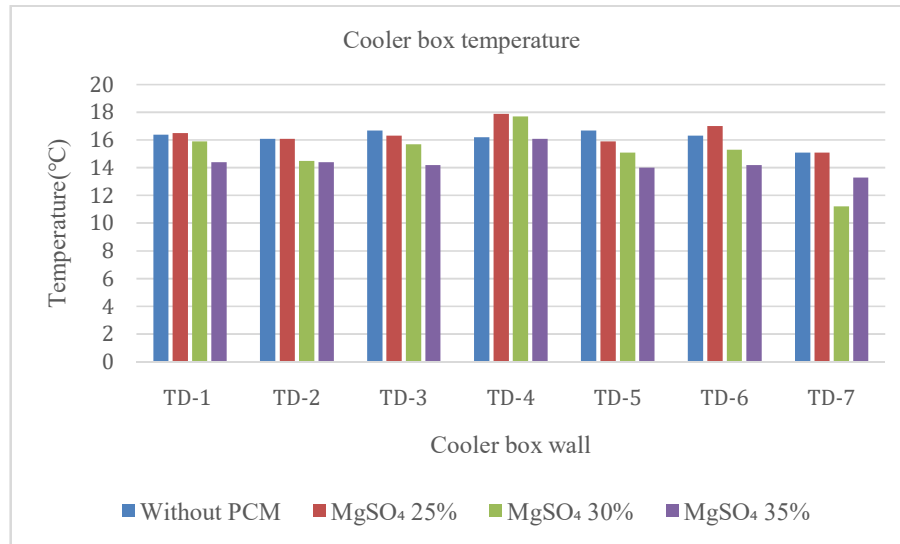


Figure8. Minimum temperature distribution of the cooler box in three days

Figure 8 shows the minimum inside temperature distribution of the cooler box using PCM with 25% MgSO<sub>4</sub>, 30% MgSO<sub>4</sub>, 35% MgSO<sub>4</sub>, and the cooler box without PCM in three days. The graph pattern tends to decrease, but there are differences in temperature in each cooler box. The most significant temperature decrease was found in the cooler box using 30% MgSO<sub>4</sub> PCM, which reached a minimum temperature of 12.7°C. This is because the 30% MgSO<sub>4</sub> PCM has a lower melting point than the others, and the physical properties of the 30% MgSO<sub>4</sub> PCM are more stable in the phase change process that crystallizes the MgSO<sub>4</sub> solution. Kore et al. (2017).

The input power from the solar panel to the cooling system in three days, can be seen in the following table.

Table2. Input power of solar panels to the cooling system

Solar panel input power(P <sub>in</sub> )(W)		
Day	P <sub>in</sub> result	Average
1	1,827.04	2,179.06
2	2,235.76	
3	2,474.38	

In the table above, it can be seen that the input power to the cooling system where there is an average input power for three days is 2,179.06 W.

Calculation of heat lost in each cooler box calculated in three days, can be seen in Table 3.

Tabel3. Heat lost

Result	Heat lost (q <sub>l</sub> ) (W)											
	Without PCM			PCM MgSO <sub>4</sub> 25%			PCM MgSO <sub>4</sub> 30%			PCM MgSO <sub>4</sub> 35%		
Per day	Day 1	Day 2	Day 3	Day 1	Day 2	Day 3	Day 1	Day 2	Day 3	Day 1	Day 2	Day 3
		58.12	62.25	60.81	61.22	60.66	61.91	83.96	85.09	84.09	72.32	73.33
Average	60.39			61.26			84.38			72.49		

Based on the table above, we can see the average heat lost during the cooling process carried out for three days. From the table, it can be seen that the average heat lost is greatest in the cooler box with 30% PCM MgSO<sub>4</sub> with heat lost of 85.09 W on the second day. Meanwhile, the lowest average heat loss in the cooler box without PCM was obtained on the first day with a heat loss of 58.12 W.

Calculation of heat load transmission in the cooler box without PCM, cooler box with PCM MgSO<sub>4</sub>, 25% cooler box with PCM MgSO<sub>4</sub> 30% cooler box with PCM MgSO<sub>4</sub> 35% for three days can be seen in Table 4.

Table4. Transmission heat load

Result	Transmission heat load (q <sub>2</sub> ) (W)											
	Without PCM			PCM MgSO <sub>4</sub> 25%			PCM MgSO <sub>4</sub> 30%			PCM MgSO <sub>4</sub> 35%		
Per day	Day 1	Day 2	Day 3	Day 1	Day 2	Day 3	Day 1	Day 2	Day 3	Day 1	Day 2	Day 3
		13.73	13.81	13.68	15.54	13.40	15.33	16.24	16.42	16.30	13.31	13.65
Average	13.74			14.75			16.32			13.58		

The table above shows the calculation results of heat transmission every day for three days. In the cooler box without PCM, the average transmission heat was 13.74 W, the cooler box with 25% PCM MgSO<sub>4</sub>, the average transmission heat was 14.75 W, the cooler box with 30% PCM MgSO<sub>4</sub>, the average transmission heat was 16.32 W, and the cooler box with 30% PCM MgSO<sub>4</sub>, the average transmission heat was 13.58 W.

The calculation of the total heat load on the cooler box for three days can be seen in Table 5.

Table5. Total cooling heat load for three days

Result	Total cooling heat load for three days (q <sub>c</sub> ) (W)											
	Without PCM			PCM MgSO <sub>4</sub> 25%			PCM MgSO <sub>4</sub> 30%			PCM MgSO <sub>4</sub> 35%		
Per day	Day 1	Day 2	Day 3	Day 1	Day 2	Day 3	Day 1	Day 2	Day 3	Day 1	Day 2	Day 3
		72.90	77.12	75.52	77.83	74.68	78.28	101.37	102.69	101.55	87.62	87.82
Average	71.18			76.93			101.87			87.26		

In the table above, the calculation results of the cooling load for three days were obtained. In the cooling box without PCM, the average cooling load is 71.18 W, PCM MgSO<sub>4</sub> 25% average cooling load is 76.93 W, PCM MgSO<sub>4</sub> 30% average cooling load is 101.87 W, and PCM MgSO<sub>4</sub> 35% total cooling load is 87.26 W.

The calculation of the coefficient of performance (CoP) of the thermoelectric cooling system can be seen in table 6.

Table6. Cooling system coefficient of performance for three days

Result	Coefficient of performance (CoP) (W)											
	Without PCM			PCM MgSO <sub>4</sub> 25%			PCM MgSO <sub>4</sub> 30%			PCM MgSO <sub>4</sub> 35%		
Per day	Day 1	Day 2	Day 3	Day 1	Day 2	Day 3	Day 1	Day 2	Day 3	Day 1	Day 2	Day 3
		0.0394	0.0341	0.0301	0.0421	0.0330	0.0312	0.0548	0.0454	0.0405	0.0474	0.0388
Average	0.0345			0.0354			0.0469			0.0402		

The table above displays the average performance coefficient of the cooling system for three days, and is obtained in the box without PCM of 0.0345, the cooling box with 25% MgSO<sub>4</sub> PCM of 0.0354, the cooling box with 30% MgSO<sub>4</sub> PCM of 0.0469, and the cooling box with 35% MgSO<sub>4</sub> PCM of 0.0402. The highest average value of performance coefficient is found in PCM 30% MgSO<sub>4</sub>. This is because the higher the concentration of MgSO<sub>4</sub>, the lower the freezing point of the solution. This is because the ions from the salt will interfere with the formation of ice crystals, lowering the freezing point of the solution. Khandagre et al. (2021). This study shows that a higher water vapor pressure of 50 mbar improves the reaction kinetics of the MgSO<sub>4</sub> dehydration process, thereby improving the performance of the material. Vasanthkumar et al. (2014).

#### 4. CONCLUSION

Based on the research that has been done, it is concluded that the minimum cooling chamber temperature in the cooling box occurs in the cooling box with 30% MgSO<sub>4</sub> PCM, which is 12.7 °C. so that the use of PCM produces lower temperatures. The highest average coefficient of performance (CoP) achieved in the cooling box with 30% PCM MgSO<sub>4</sub> is 0.0469 and the CoP of the cooling box without PCM is 0.0345. So the use of PCM



MgSO<sub>4</sub> can increase the coefficient of performance of solar-powered thermoelectric cooling systems. In this study, 30% MgSO<sub>4</sub> PCM is most appropriate to be used as PCM because it affects the minimum temperature of the cooling chamber and the cooling system performance coefficient. This is because the higher the concentration of MgSO<sub>4</sub>, the lower the freezing point of the solution, and of the solar cell also have an effect on the performance of the cooling box.

## REFERENCES

- Akbar, I., Malik, A., Aziz, A., Faritzie, H.AI, Rawani, D., Analysis of tortuosity effect on porous heatsink on natural convection heat transfer, *Journal of Mechanical Engineering*, 23(2), 41–48, 2023.
- Akbar, M., Rizal, T.A., Syntia, R., Testing the cooling performance of thermo electric cooling (tec) using heatsinks with dimensional variations and material types, *JURUTERA-General Journal of Applied Engineering*, 8(01), 19–28, 2021.
- Biwole, P., Eclache, P., Kuznik, F., Improving the performance of solar panels by the use of phase-change materials, *Proceedings of the World Renewable Energy Congress–Sweden*, 8–13 May, 2011, Linköping, Sweden, 57, 2953–2960, 2021.
- Cengel, Y.A., Ghajar, A.J., *Heat and mass transfer fundamentals & applications in analytical biochemistry*, 11(1), 2015.
- Durganjali, C.S., Bethanabhotla, S., Kasina, S., Radhika, D.S., Recent developments and future advancements in solar panels technology, *Journal of Physics: Conference Series*, 1495(1), 2020.
- Ferreira, A.P., Zhou, M., Bock, S., Childers, B., Melhem, R., Mossé, D., Increasing pcm main memory lifetime, *Proceedings -Design, Automation and Test in Europe, DATE*, 914–919, 2010.
- Fikry Ar Rasyid, A., Aqil Maulana, Y., Akbar Nafis, T., Hadi Setiawan, E., Effect of load addition on solar powered thermoelectric cooling system, *Manufacturing Energy Engineering Journal*, 9(1), 2528–3723, 2024.
- Harahap, P., Effect of solar panel surface temperature on the power generated from different types of solar cells. *RELE (Electrical and Energy Engineering): Journal of Electrical Engineering*, 2(2), 73–80, 2020.
- Khandagre, M., Gupta, B., Bhalavi, J., Baredar, P., Magnesium sulfate heptahydrate as phase change material in double slope solar still, *Journal of Thermal Engineering*, 7(2), 196–214, 2021.
- Kore, B.P., Pardhi, S.A., Dhoble, N.S., Dhoble, S.J., Swart, H.C., Luminescence characterization of dy and eu doped na6mg(so4)4 phosphors, *Luminescence*, 32(4), 564–572, 2017.
- Pomianowski, M., Heiselberg, P., Zhang, Y., Review of thermal energy storage technologies based on pcm application in buildings. *Energy and Buildings*, 67, 56–69, 2013.
- Puspita, S.C., Sunarno, H., Indarto, B., Thermoelectric generator for battery charging. *Journal of Physics and its Applications*, 13(2), 84, 2017.
- Rifky, R Sirodz, Y., Development of a solar powered city car cabin cooling model using photovoltaics (pv) and thermoelectric (tec). *Teknobiz: Scientific Journal of Master Study Program*, 10(1), 34–40, 2020.
- Salsa hayani, F., Stefanie, A., Bangsa, I.A., Hybrid thin film solar panel thermoelectric generator sf 170-s cis 170 watt at 1 mw cirata solar power plant, *Journal of Electrical Engineering Uniba*, 6(1), 154–160, 2021.
- Salsabila, F., Manunggal, B.P., Yuliani, I., Manufacture of cooling box for storage of sinovac vaccine based on thermoelectric. *Industrial Research Workshop and National Seminar*, 12(1), 907–914, 2021.
- Setiawan, B., Sutopo, E., Design of cold box in beef cooling system with 50 kg capacity, *National Seminar of Science and Technology*, 16, 1–10, 2019.
- Sharpe, L., Burhanuddin, N., Majcan, T., Rebolledo, J., Increasing the efficiency of a peltier device by assessing the thermal performance of liquid-cooled microchannel heat ssnks, *PAM Review Energy Science & Technology*, 7, 3–22, 2020.
- Silaban, M., Solar thermal utilization in wood drying process, *Journal of the Center for Energy Technology (B2TE)*, 7 (1), 1–8, 2013.
- Suryana, D., Ali, M.M., The effect of temperature on voltage produced by monocrystalline solar panel (case study : baristand industry surabaya), *Journal of Process Technology and Industrial Innovation*, 2(1), 49–52, 2016.
- Susilo, R.T., Hermawan, R., Analysis of cooling capacity in the appearance quality inspection dome room at pt xxx, *SEMSRESTEK Journal*, 2020.
- Tyagi, V.V., Buddhi, D., Pcm thermal storage in buildings: a state of art, *Renewable and Sustainable Energy Reviews*, 11(6), 1146–1166, 2007.
- Vasanthkumar, P., Ilandje, R., Pachaiyappan, S., Experimental analysis of thermal energy storage system using inorganic pcm for hvac applications, *International Journal of Engineering Science & Advanced Technology*, 4(1), 102–108, 2014.